Comparison of GOES Cloud Classification Algorithms Employing Explicit and Implicit Physics

RICHARD L. BANKERT AND CRISTIAN MITRESCU

Naval Research Laboratory, Monterey, California

STEVEN D. MILLER

Cooperative Institute for Research in the Atmosphere, Colorado State University, Fort Collins, Colorado

ROBERT H. WADE*

Science Applications International Corporation, Monterey, California

(Manuscript received 25 August 2008, in final form 10 February 2009)

ABSTRACT

Cloud-type classification based on multispectral satellite imagery data has been widely researched and demonstrated to be useful for distinguishing a variety of classes using a wide range of methods. The research described here is a comparison of the classifier output from two very different algorithms applied to Geostationary Operational Environmental Satellite (GOES) data over the course of one year. The first algorithm employs spectral channel thresholding and additional physically based tests. The second algorithm was developed through a supervised learning method with characteristic features of expertly labeled image samples used as training data for a 1-nearest-neighbor classification. The latter's ability to identify classes is also based in physics, but those relationships are embedded implicitly within the algorithm. A pixel-to-pixel comparison analysis was done for hourly daytime scenes within a region in the northeastern Pacific Ocean. Considerable agreement was found in this analysis, with many of the mismatches or disagreements providing insight to the strengths and limitations of each classifier. Depending upon user needs, a rule-based or other postprocessing system that combines the output from the two algorithms could provide the most reliable cloud-type classification.

1. Introduction

Automated cloud-type classification in satellite imagery is a valuable resource in both the operational and research communities. Cloud classifier output provides useful information to researchers and operational users alike. In an instantaneous sense, knowledge of cloud types in a given scene improves the retrieval of cloud parameters (e.g., by providing a priori information on liquid/ice/mixed phase). When analyzed over a long time period this knowledge contributes to the analysis of radiation and heat budgets, which are impacted differently depending upon the cloud types (Li et al. 2007). Owing to the importance of clouds in climate feedback processes, an improved understanding of cloud-type distribution and its change over time would benefit climate research (Wang and Sassen, 2001). Important operational uses of cloud-type classification include the identification of convective clouds over oceanic regions, where observational data are sparse (Donovan et al. 2008). In addition to the identification of convective clouds, diagnosing areas of fog/stratus and supercooled liquid clouds would positively impact aviation route planning.

To determine the cloud type of a pixel or group of pixels in satellite imagery, an appropriate classification algorithm must be selected. Algorithm choice is driven in part by the cloud types of interest and the intended use(s) of the output. These algorithms can, in general, be grouped into theoretical/physical (explicit physics,

* Deceased.

Corresponding author address: Richard Bankert, Naval Research Laboratory, 7 Grace Hopper Ave., Monterey, CA 93943-5502.
E-mail: rich.bankert@nrlmry.navy.mil

DOI: 10.1175/2009JAMC2103.1

Report Documentation Page

Form Approved
OMB No. 0704-0188

1. REPORT DATE	2. REPORT TYPE	3. DATES COVERED
2009		**00-00-2009 to 00-00-2009**

4. TITLE AND SUBTITLE	5a. CONTRACT NUMBER
Comparison of GOES Cloud Classification Algorithms Employing Explicit and Implicit Physics	5b. GRANT NUMBER
	5c. PROGRAM ELEMENT NUMBER
6. AUTHOR(S)	5d. PROJECT NUMBER
	5e. TASK NUMBER
	5f. WORK UNIT NUMBER
7. PERFORMING ORGANIZATION NAME(S) AND ADDRESS(ES) **Naval Research Laboratory,Monterey,CA**	8. PERFORMING ORGANIZATION REPORT NUMBER
9. SPONSORING/MONITORING AGENCY NAME(S) AND ADDRESS(ES)	10. SPONSOR/MONITOR'S ACRONYM(S)
	11. SPONSOR/MONITOR'S REPORT NUMBER(S)

12. DISTRIBUTION/AVAILABILITY STATEMENT
Approved for public release; distribution unlimited

13. SUPPLEMENTARY NOTES

14. ABSTRACT

15. SUBJECT TERMS

16. SECURITY CLASSIFICATION OF:			17. LIMITATION OF ABSTRACT	18. NUMBER OF PAGES	19a. NAME OF RESPONSIBLE PERSON
a. REPORT **unclassified**	b. ABSTRACT **unclassified**	c. THIS PAGE **unclassified**	**Same as Report (SAR)**	**12**	

hereinafter referred to as EP) or empirical/statistical (implicit physics, hereinafter referred to as IP) methods. Recent research in the related areas of scene classification and cloud property retrievals is summarized in the next section.

Validation of an individual classifier applied to real-time or unlabeled testing data is difficult given the lack of independent validation data. The objectives of the research described here are to validate and identify the strengths and limitations of two classifiers, one based on EP methods and the other based on IP methods, through comparison of their output. *Geostationary Operational Environmental Satellite-11* (*GOES-11*; 135°W lon) data over a 1-yr period serve as the dataset. This comparison requires a reconciliation of the various cloud categories defined in each of the algorithms. Although neither classifier output should be considered to be "truth," classifier agreement can enhance the confidence in the output of both classifiers. The purpose of this research is to document agreements and to explain the disagreements between the two algorithms. Future research will apply this analysis to the refinement of current algorithms or development of new ones.

The EP cloud-type algorithm is described in section 3, and the IP algorithm is described in section 4. Comparison results and analysis are presented in section 5, followed by a summary discussion in section 6.

2. Related research

Many examples of both EP and IP approaches, applied to various sensor data for a variety of classification problems, can be found in the research literature. The EP algorithms relate the spectral and spatial contrasts observed in multispectral imagery to characteristics of various cloud types. For example, the spatial variation in visible reflectance or infrared brightness temperature provides textural information for differentiating, for example, stratus and stratocumulus cloud fields. Absolute thresholds in temperature or reflectance provide information on the height and/or opacity of the cloud that help to relate it to a classification. Differential optical properties can also be exploited, such as the "split window" difference for detecting thin cirrus clouds. Coupling that information with visible reflectance provides a means to detect thin cirrus overlapping lower-level cloud (Heidinger and Pavolonis 2005). Still other channel combinations enable the distinction among liquid, ice, and supercooled or mixed phase cloud-top conditions. These and other techniques as applied to EP cloud masking and typing are described by Pavolonis and Heidinger (2004).

Research has also been done on testing the capability of the Visible/Infrared Imager Radiometer Suite (VIIRS) cloud mask algorithm as applied to Moderate Resolution Imaging Spectroradiometer (MODIS) data (Hutchison et al. 2005). The MODIS cloud mask is discussed in Ackerman et al. (2008). Using a grouped threshold approach in addition to the application of radiative transfer modeling, cloud detection and classification algorithms were developed for Advanced Very High Resolution Radiometer (AVHRR) data in Dybbroe et al. (2005). Earlier work applying a grouped threshold method, with the aid of radiative transfer calculations, to AVHRR scene identification is discussed by Baum and Trepte (1999). Wang and Sassen (2001) describe a physically based algorithm developed and applied to ground-based remote sensors. Cloud type and macrophysical cloud properties were identified. Directly related to this research, cloud property retrieval algorithms from GOES data are described in Mitrescu et al. (2006).

Machine learning techniques have been applied to various image classification problems for many years. A majority of these classification tasks are approached as supervised learning problems, in which previously classified samples from a historical dataset are represented by a characteristic feature vector and serve as a set of training samples. Mazzoni et al. (2007) apply a supervised learning technique in the form of support vector machines to scene classification within Multiangle Imaging Spectroradiometer (MISR) data. Baldwin et al. (2005) apply a nearest-neighbor algorithm to the classification of rainfall systems in radar data. The training sets were class labeled using cluster analysis, an unsupervised learning method, as opposed to being manually labeled. Parikh et al. (1997) apply neural networks, genetic algorithms, and statistical methods to the recognition and tracking of midlatitude cloud systems in cloud-top pressure datasets. Baum et al. (1997) use labeled AVHRR samples to train a fuzzy logic cloud classifier.

Classification and retrieval schemes have also been developed using a combination of EP and IP. Oceanic convective cloud diagnoses are performed using a fusion of output from a 1-nearest-neighbor cloud classifier (Bankert and Wade 2007) and a thresholding technique for deep convection (Schmetz et al. 1997; Mosher 2002) to produce an enhanced product (Donovan et al. 2008). Li et al. (2007) compare different satellite sensors (present and future) in cloud classification using the MODIS cloud mask as the initial classification for a maximum likelihood classification procedure (unsupervised learning). Seemann et al. (2003) apply a statistical retrieval algorithm in combination with a nonlinear physical retrieval algorithm to MODIS data in the retrieval of atmospheric temperature and moisture distribution, total column ozone, and surface skin temperature. Fouilloux and Iaquinta (1998) present an AVHRR cloud classification

TABLE 1. Cloud type outputs given by the "explicit physics" classification algorithm.

Clear (Clr)
Partly cloudy
Liquid water (Liq)
Supercooled water or mixed phase (Mix)
Glaciated–opaque ice (Glac)
Cirrus (Ci)
Cloud overlap (OL)

algorithm based on physical and textural properties used in combination with neural networks for the extraction of cloud optical thickness and droplet effective radius.

3. Cloud-type algorithm—Explicit physics

Based on the research described in Pavolonis et al. (2005), Pavolonis and Heidinger (2004), and Mitrescu et al. (2006), an EP algorithm to determine the cloud type of a given cloudy pixel in GOES imagery is developed. This EP classifier provides a front-end filter for locating and identifying the appropriate cloud-top-properties retrieval algorithm. Using a series of thresholding tests on all five GOES imager channels, each pixel is assigned one of the cloud types listed in Table 1. Pixels classified as partly cloudy are ignored for this study. The algorithm was incorporated into the Naval Research Laboratory (NRL) automated processing system and coupled to the Navy Operational Global Atmospheric Prediction System for auxiliary data requirements.

Using a cloud mask algorithm (Heidinger 2004) that includes spatial uniformity information, a pixel is first determined to be clear (no cloud), partly cloudy, or cloudy. For cloudy pixels, a test for semitransparent ice cloud overlapping liquid water droplet cloud (Pavolonis and Heidinger 2004) is performed. This test checks the behavior of the visible channel reflectance and the 11- and 12-μm brightness temperature difference (split window). A cirrus (Ci) test for transmissive (optically thin) ice clouds, as described in Pavolonis et al. (2005), is also applied. Both the overlapping test and thin cirrus test are designed to minimize the false alarms of each type; therefore, one would expect occasional misclassifications when Ci or overlapping clouds are present. If both of these tests fail, the appropriate (as determined by the 11-μm channel brightness temperature) cloud phase tests for 1) liquid water—brightness temperature greater than 273 K, 2) supercooled water or mixed phase—composed entirely of supercooled water droplets or both ice and supercooled, and 3) glaciated (optically thick ice) clouds—entirely ice crystals or glaciated tops (e.g., deep convection)—are applied and the pixel's cloud type is assigned.

TABLE 2. Classes used in cloud classifier (implicit physics).

Stratus (St)
Stratocumulus (Sc)
Cumulus (Cu)
Altocumulus (Ac)
Altostratus (As)
Cirrus (Ci)
Cirrocumulus (Cc)
Cirrostratus (Cs)
Cumulus congestus (CuC)
Cumulonimbus (Cb)
CsAn—Cs near turret in thunderstorm; more closely related to deep convection than "garden variety" Cs
Clear (Clr)
Ground snow (Sn)
Haze (Hz)
Sun glint (Sg)

4. GOES cloud classifier—Implicit physics

Using a supervised learning method that was first applied to AVHRR data (Tag et al. 2000), an IP cloud classifier has been developed and further refined for application to GOES data (Bankert and Wade 2007). A training dataset is established through independent expert agreement of thousands of labeled 16 $\times$ 16 pixel samples. The classes used by the experts are listed in Table 2. In addition to the imagery, the experts had synoptic weather charts and other data available to assist in the class assignment of each training sample. General cloud identification is one use of the classifier, but more specific or application-driven uses are possible. The IP cloud classifier is currently being used for an oceanic convective diagnosis and nowcasting system (Kessinger et al. 2009). Other potential uses include snow/cloud delineation and low-cloud or thin cirrus detection, depending upon any given user's specific needs or application.

Each expert-labeled training set sample is represented by a vector of characteristic features computed or extracted from each spectral channel with a final subset of features (Bankert and Wade 2007) chosen through a feature selection routine (Bankert and Aha 1996). Various training sets were established, differentiated by satellite (GOES-East or GOES-West), sea or land, and daytime or nighttime scenes. For this research, GOES-West land day and GOES-West sea day training sets are used within a 1-nearest-neighbor classifier. Daytime observations offer an increased number of classes because of the availability of visible-band data. The minimum distance in feature space between an unclassified sample presented to the classifier and the training data samples is found, and the class label of the nearest-neighbor training sample is subsequently assigned to each pixel in the unclassified sample.

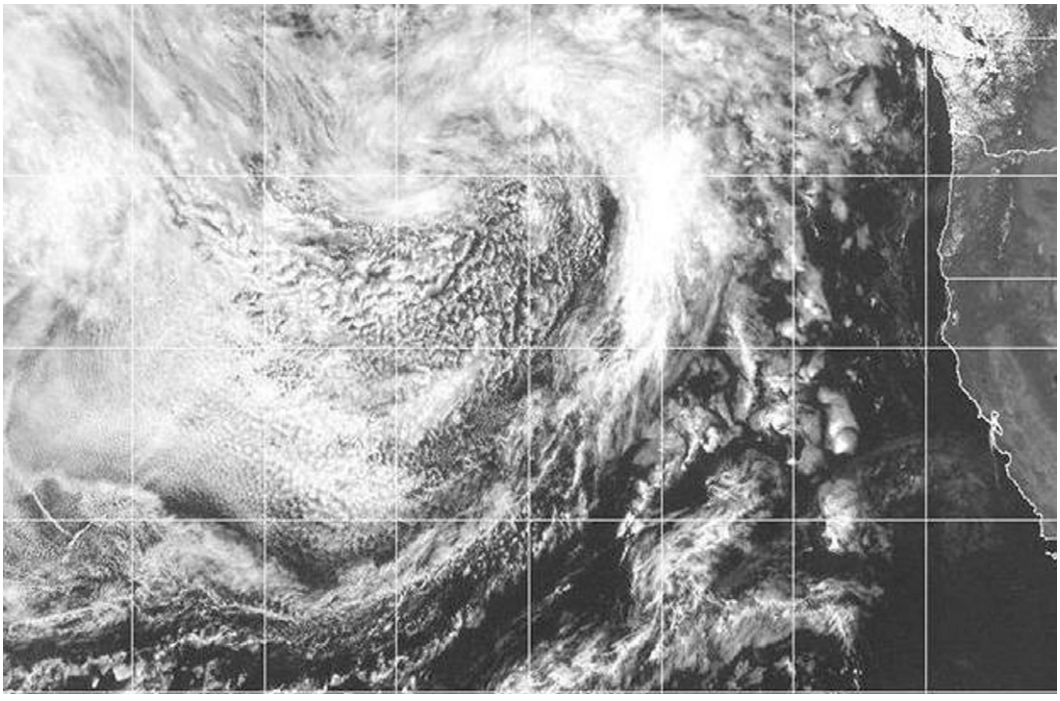

FIG. 1. *GOES-11* visible image depicting the region used for the comparison study.

As described in Tag et al. (2000), classifications of overlapping boxes (a 16 × 16 pixel window is applied every 8 pixels) within each image are performed. Each image pixel in a given 16 × 16 pixel box is assigned the same class, resulting in every pixel being classified four times (excluding image edges). The majority class is assigned (ties broken randomly) to each pixel, followed by a postprocessing routine that applies conservative measures to check the classification validity of each pixel. The use of texture measures within the feature set and the use of overlapping boxes help to overcome some of the limitations associated with pixel-based classifications and provide a more robust classification. Given the class types used in this IP algorithm, single pixel spectral information alone would not have provided satisfactory results. Because each box is assigned a specific class, no ''multiple,'' ''overlapping,'' or ''unknown'' class is used. For this analysis, pixels classified as ground snow, haze, and sun glint are ignored.

5. Algorithm comparison analysis

The EP and IP algorithms were applied to hourly daytime *GOES-11* data for a 1-yr period (from October 2006 to October 2007) in the northeastern Pacific Ocean (Fig. 1). Both algorithms define a pixel as daytime if the solar zenith angle is below a specified threshold. To simplify the pixel comparison between the two classifiers, the IP classes are combined to form a set of classes that match the EP cloud classes. This clustering of classes is summarized in Table 3. Note that no overlapping cloud class is possible with the IP algorithm. Because the method and criteria used to define the classes for each classifier are different, these clusters are not perfect matches for all pixels. However, analysis of the comparisons should provide an indication as to whether disagreements are a result of algorithm limitations, class definitions, or a combination of the two.

More than 1.4 billion classified pixel pairs (from 4295 *GOES-11* images) were compared over the year-long test period. A percentage distribution of all possible

TABLE 3. The IP class clusters used for comparisons with EP cloud types.

Liquid water
Stratus (St)
Stratocumulus (Sc)
Cumulus (Cu)
Mixed phase/supercooled water
Altocumulus (Ac)
Altostratus (As)
Cumulus congestus (CuC)
Glaciated
Cirrocumulus (Cc)
Cirrostratus (Cs)
Cumulonimbus (Cb)
CsAn
Clear (Clr)—not combined
Cirrus (Ci)—not combined

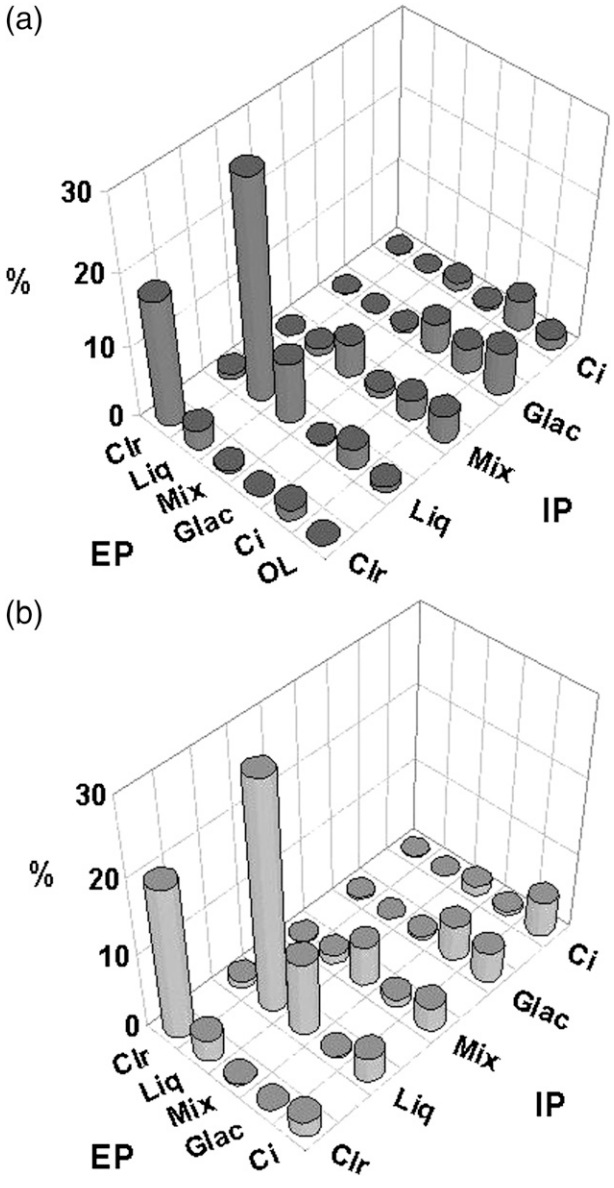

FIG. 2. (a) Percent frequency of occurrence, over entire dataset, of each possible pixel classification combination for the two algorithms (EP and IP). (b) As in (a) after removing all OL samples.

combinations for classifications within the two classifiers is presented in Fig. 2a. Most of the higher percentages (greater than 2% of the total pixels) of mismatches or disagreements occurred with pixels classified by the EP algorithm as either cirrus (Ci) or overlap (OL). The lack of an OL class in the IP classifier is an obvious explanation for this part of the distribution. A higher total percentage of Ci samples in the EP algorithm classifications (14.9%), relative to the IP classifier (7.3%), is a result of limitations in the IP algorithm and will be discussed later. To get a more direct comparison on the

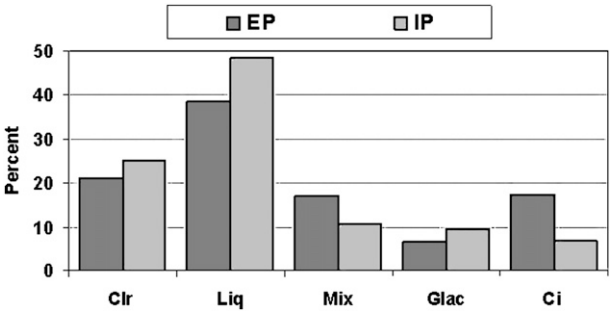

FIG. 3. Percentage distribution of total pixels for the classes within each classifier, disregarding OL pixels.

"cloud climatology" for this region produced by each algorithm, all pixels classified as OL by EP are removed from the distribution matrix to produce the same set of classes for each algorithm and the probability distribution is recomputed. These results are presented in Fig. 2b, with total percentages for each class shown in Fig. 3. The IP classifier has a higher preference for liquid and glaciated clouds, whereas the EP algorithm prefers mixed (supercooled water droplets) and Ci clouds as compared with the IP classifier. The discrepancy in the number of Ci samples between the two algorithms stands out.

Other summaries of the pixel-to-pixel comparisons over the entire dataset can be found in Figs. 4a and 4b. The percent distributions of all pixels over the entire year within a specific EP cloud class and the coincident IP cloud class (as defined in Table 3) are displayed in Fig. 4a. For example, 57.2% of the pixels classified as mixed phase or supercooled water by the EP algorithm were classified as one of the liquid IP cloud classes. Figure 4b is a graph of the percent distributions within an IP class and the coincident EP cloud type.

As evident in Fig. 4, a considerable amount of agreement exists between the EP and IP classifiers. A significant exception is the high percentage of pixels classified as supercooled (or mixed) by the EP algorithm and as one of the liquid water cloud classes by the IP algorithm. A discussion for that specific disagreement follows below. The most notable agreements, with the highest percentages, are within the clear (no cloud) and liquid water cloud classes, which also have the highest frequency of occurrence within the entire dataset (Fig. 2). Although classifier agreement increases confidence in each classifier output, some of the disagreements are a result of the different original class compositions and how those classes were defined. Therefore, neither classifier may actually be in error for certain situations. A further analysis of the results, along with knowledge of each algorithm's strengths and limitations, led to the following observations for specific notable disagreements:

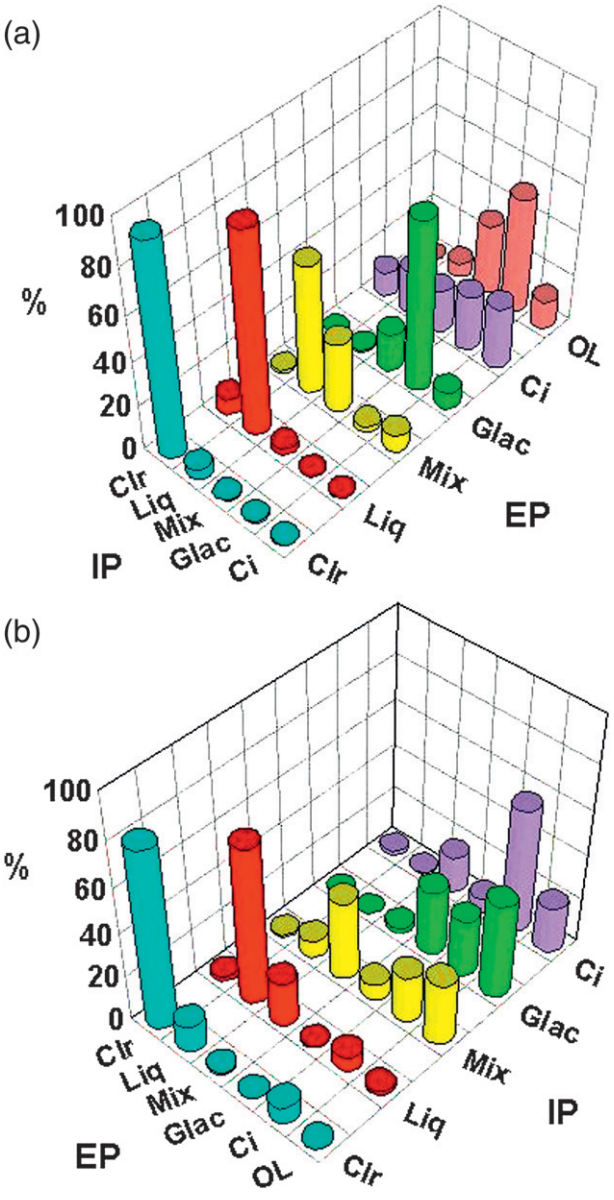

FIG. 4. (a) Percent distribution of pixels within each EP cloud type as classified by the IP classifier; EP axis columns sum to ~100%. (b) Percent distribution of pixels within each IP cloud class as classified by the EP classifier; IP axis columns sum to ~100%.

1) IP = liquid (St, Sc, Cu) and EP = supercooled (or mixed): Greater than one-half of the EP supercooled pixels were paired with IP liquid cloud classifications. Some cases reflect a known bias of EP toward higher supercooled water or mixed phase type. The frequent occurrence of clouds generated in cold air masses that pass over the Pacific results in most of these mismatches. Figure 5 is presented as an example. The cloud tops are too cold to meet the threshold for liquid clouds in the EP algorithm (Fig. 5b). Physics allows for these clouds to be composed of liquid water droplets, but in a supercooled state. The training set of the IP classifier (Fig. 5a) contains similar cold-air cloud samples that were classified as Cu and Sc by the experts because of the estimated cloud height. Therefore, based on the class definitions for each algorithm, no misclassification occurs in either classifier. Similar to this situation are pixels classified as "mixed" by IP and "glaciated" by EP. These pixels could be actual midlevel atmosphere clouds (defined as As and Ac within the IP classifier) with glaciated or very cold tops. Less frequent is that this situation could be a result of very thin Ci overlapping a low cloud deck (i.e., the OL cloud type). The thin Ci signal is missed by the IP classifier and the test for OL cloud type fails in the EP algorithm, most likely because of the split-window threshold not being exceeded. The pixel is then classified by EP as supercooled water.
2) IP = mixed (As or Ac) and EP = overlap: The IP algorithm does not output an OL class; therefore, actual OL pixels are being classified as As or Ac (Fig. 5a; white oval) with signals from both low cloud and overlying Ci being used to give a mixed phase classification as found in the nearest-neighbor training data. In Fig. 5 (white oval), thin high clouds are streaming over the low clouds associated with the front.
3) IP = liquid and EP = Ci: Two aspects of the IP algorithm negatively affect its ability to classify Ci correctly. Either the classification assignment method (in which all pixels in a given box are classified as the same class) or the postprocessing check of IR brightness temperature for initially classified Ci samples (performed to lower the number of Ci false alarms) leads to a misclassification in the IP. Also, these could be OL pixels that are missed by both methods (see Fig. 6: area enclosed by black oval). Here the OL test fails in the EP algorithm but the Ci test confirms the presence of thin high clouds (e.g., Fig. 6b). For this type of disagreement, based on either reasoning, one would expect Ci to be present in the pixel.
4) IP = mixed and EP = Ci: Examples found in the dataset imply that both classifiers are missing OL type for this situation. The IP algorithm is getting signals from both types (e.g., Fig. 6a; white oval) and classifying the pixel as mixed phase (As or Ac), and the OL test fails and the Ci test passes in the EP algorithm (e.g., Fig. 6b; white oval).
5) IP = Ci and EP = supercooled (or mixed): Although not nearly as prevalent as the opposite situation (observation type 4), Ci (or OL type) is missed by the EP classifier but Ci is detected by the IP classifier.

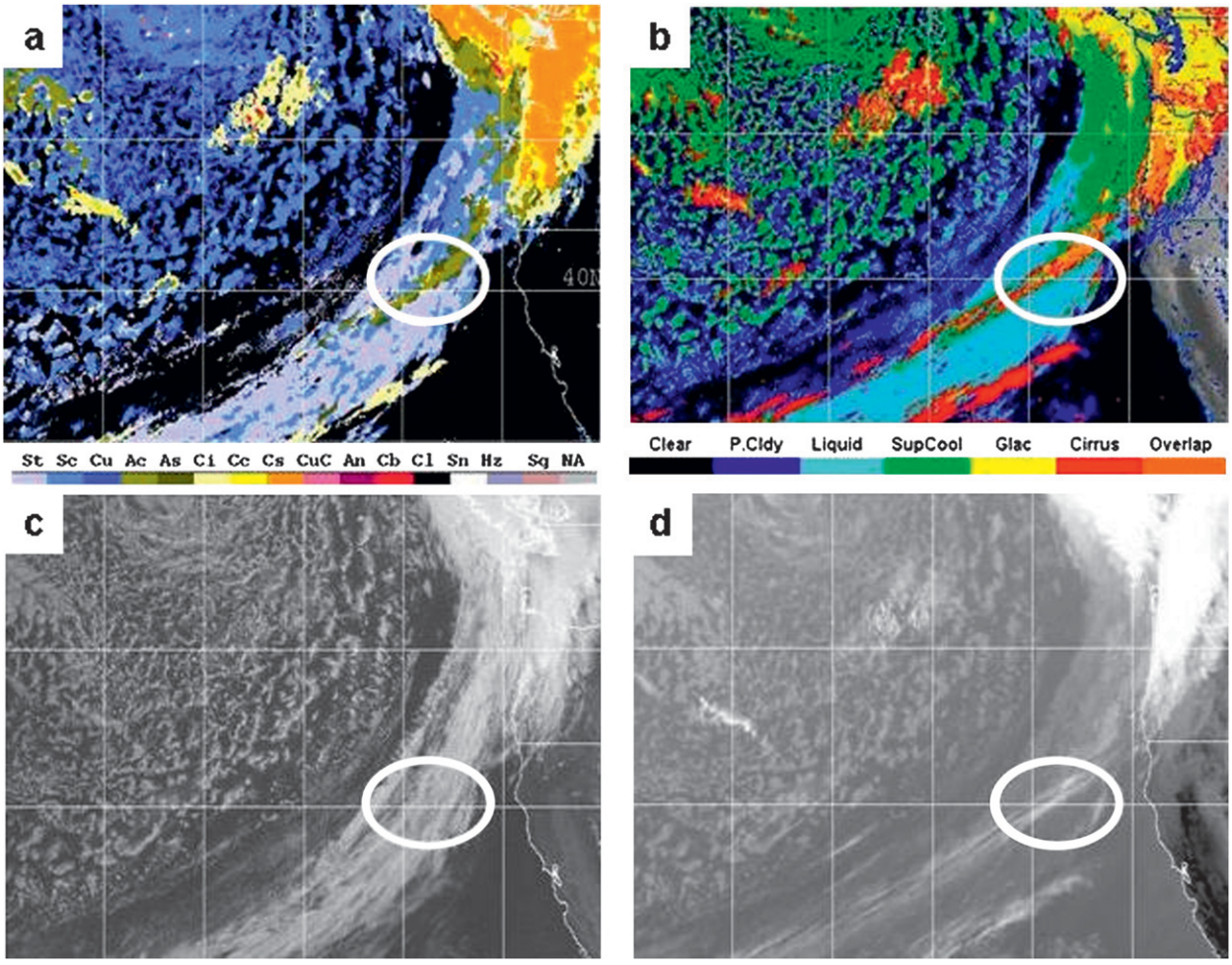

FIG. 5. Example case (1700 UTC 16 Apr 2007) of (a) IP classification of low clouds (St, Sc, and Cu; blue colors) and (b) EP classification of supercooled (mixed) clouds (green) for the same pixels, mainly in cold air behind the front. (c) *GOES-11* visible image and (d) IR image are also provided for reference.

Actual OL could also be misclassified as Ci by the IP classifier. Figure 7a (area within black oval) provides an example in which an overlapping cloud situation is misclassified as Ci by IP (which has no OL class) and the same area in Fig. 7b is classified as supercooled water or mixed phase by EP. Again, regardless of whether the actual classification is Ci or OL, thin high clouds are known to be present in the pixel.

6) IP = clear and EP = liquid: The IP algorithm can miss thin low-cloud pixels near the terminator (high solar zenith angle) resulting in a clear (no cloud) classification. In some instances, the IP postprocessing check (for the minimum visible channel albedo threshold for cloud detection) can change an original liquid cloud class to clear or there could be low thin clouds misclassified as clear (e.g., Fig. 8a; black oval).
7) IP = Glac and EP= Ci or OL: These pixel pair classification outputs are most likely the result of class definitions (particularly with regard to optical thickness for Ci), lack of OL class in IP, and classifier design rather than misclassifications. Of interest is that more pixels classified by the IP algorithm as cirrostratus and cirrocumulus were paired with EP classification of OL than Glac, whereas pixels classified by IP as cumulonimbus and CsAn (see Table 2) had a higher frequency pairing with Glac than OL. These distributions are indicative of the optical thickness of the clouds (e.g., manifesting in magnitude of visible reflectance) as used indirectly in the class definitions.

6. Discussion

In the ideal case, the validation of a cloud classification algorithm would involve a truth dataset of cloud types to match against the classifier output. The truth dataset could be constructed from a satellite interpretation

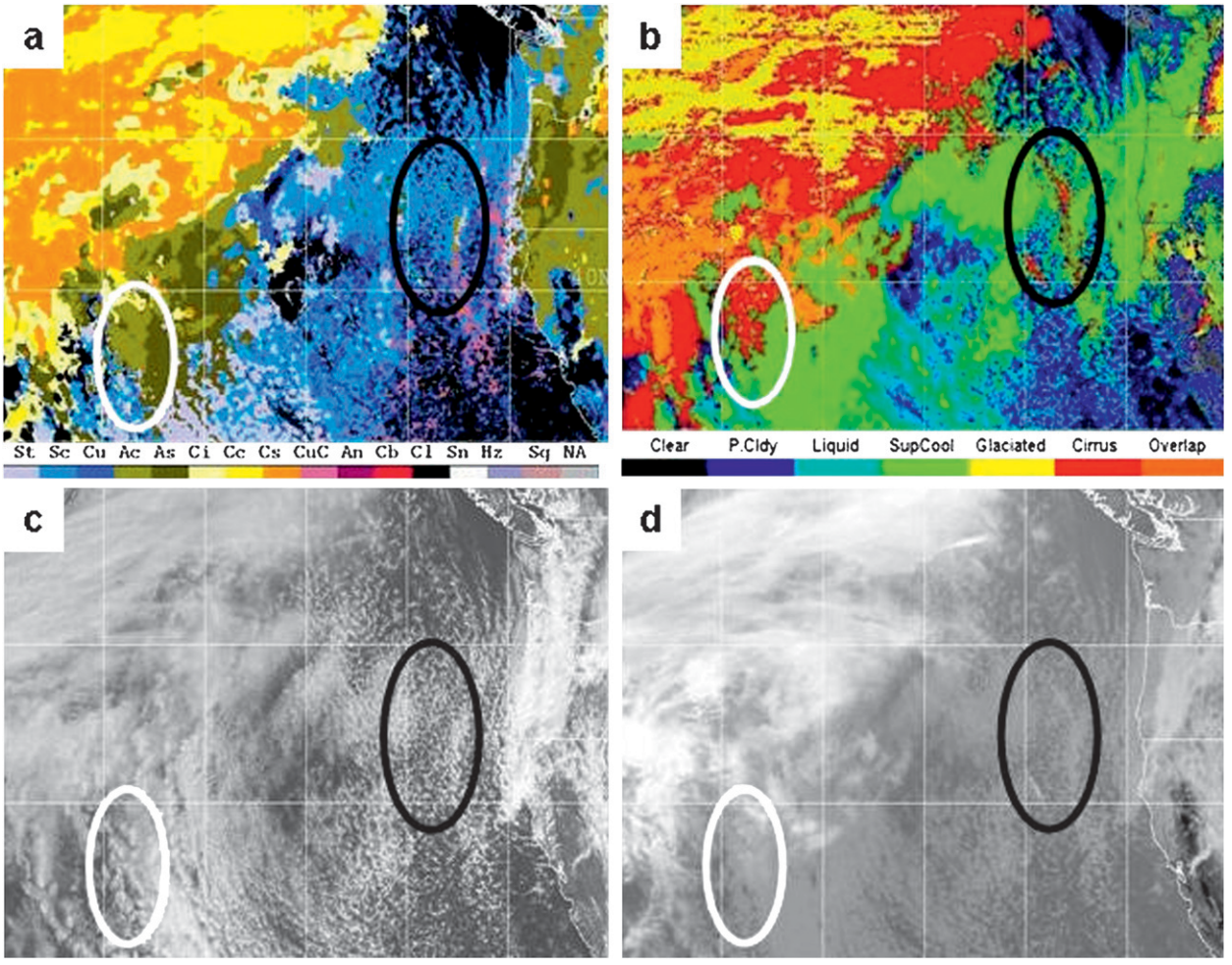

FIG. 6. The 1900 UTC 27 Mar 2007 (a) IP classification, (b) EP classification with (c) *GOES-11* visible channel and (d) IR channel images.

expert's analysis and/or through further consensus with more specialized satellite observations [e.g., active sensors such as *CloudSat* and Cloud–Aerosol Lidar and Infrared Pathfinder Satellite Observation (CALIPSO)]. Although developing truth data was not practical and no other observational datasets were available for validating the classifiers in the current study, comparing the output of each classifier with knowledge of their respective strengths and limitations leads to a more complete understanding of performance. Future efforts, especially those with a more limited time period and areal coverage, connected with field campaign observations will provide opportunities along these lines.

Many of the classifier disagreements, as noted in this study, are a result of the lack of an OL cloud class in the IP algorithm and/or missed OL cloud types in the EP algorithm. By enlisting active sensor data (*CloudSat* and CALIPSO), adding OL samples to IP training data, and, if necessary, developing new discriminating features, it is possible to improve the IP classifier performance in these situations. Alternatively, a postprocessing check on specific pixels (e.g., As and Ac pixels) to determine if an overlapping cloud situation exists could also be implemented. For the EP algorithm, an adjustment to the OL test, which is designed to minimize false alarms, would lower the frequency of misses by this classifier. Again, such adjustments may enlist other observing systems such as *CloudSat*, CALIPSO, or the 1.38-μm band on MODIS. These potential improvement examples to each algorithm were only revealed through the current comparisons.

A problem with both classifiers—in particular, in the IP classifier—is the misclassification of actual Ci pixels because both algorithms are designed conservatively to minimize the number of false alarms of Ci. Slight modifications could be made to either or both Ci tests (postprocessing part of the IP algorithm) to lower the number of misclassifications. Modifications should be applied such that false alarms are not significantly increased.

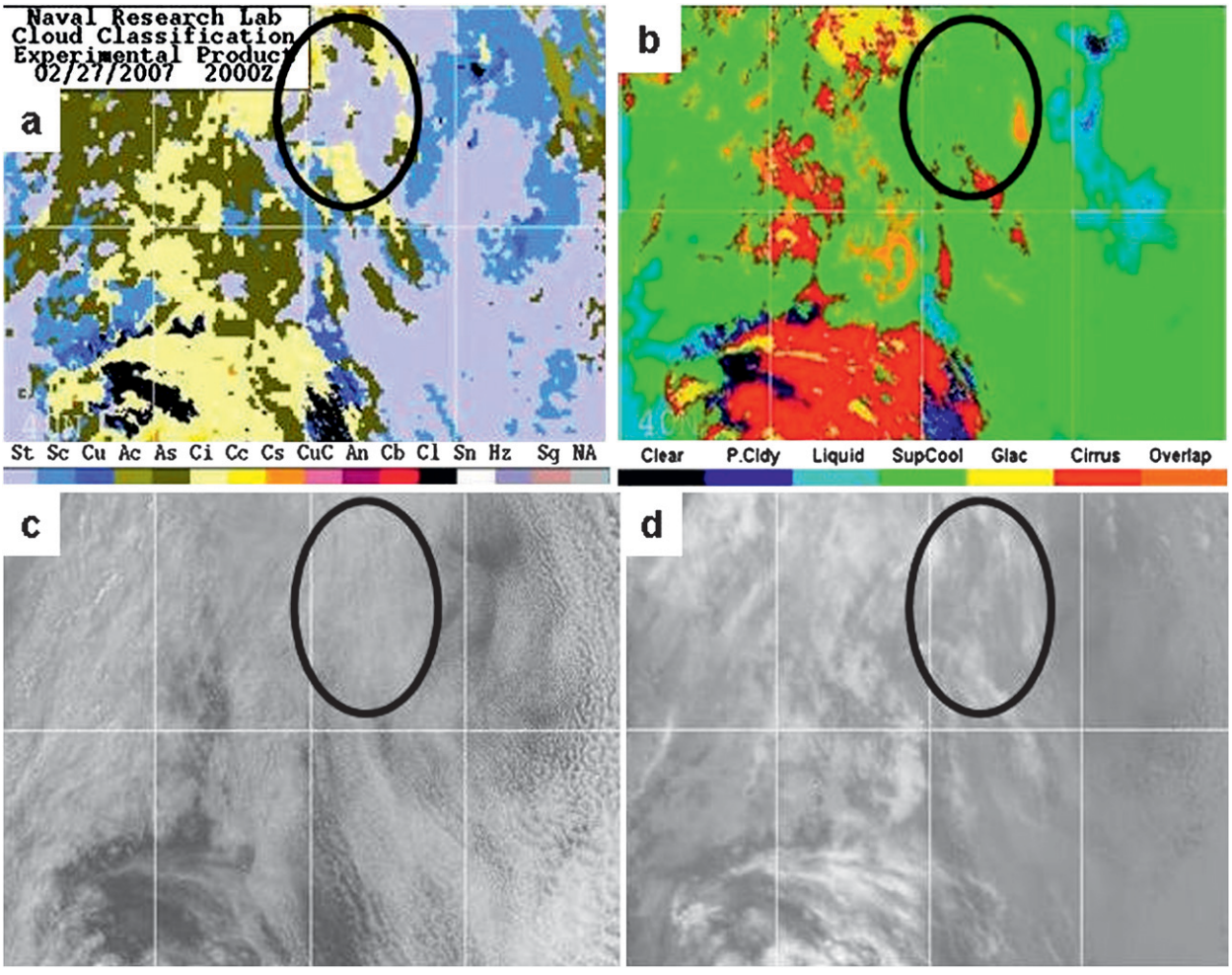

FIG. 7. Example case (2000 UTC 27 Feb 2007) of (a) IP classification of Ci and (b) EP classification of mixed (supercooled) clouds for the same pixels. (c) *GOES-11* visible image and (d) IR image are also provided for reference.

Development of a hybrid cloud classification algorithm based on both the IP and EP algorithms would also overcome the OL and Ci problems in addition to other limitations. This "classification adjustment" algorithm could take the form of a rule set applied to each pixel. Pixels that have agreement in class label would be unchanged, with specific rules applied to those pixels in disagreement. For example, if IP assigns a mixed-phase class and EP is OL, the pixel is classified as OL (rule determined through this comparison research). Another example would be that if a pixel is assigned a mixed phase class from the IP algorithm and Ci from the EP algorithm the pixel is given a final classification of OL. Because of the possibility of more than one explanation for a specific disagreement, other rules or threshold checks would be necessary. User needs and knowledge depth of classifier limitations would ultimately aid in determining whether just one of the individual classifiers was sufficient or whether a customized combination of the two algorithms should be applied.

Acknowledgments. The current research effort is funded by the National Aeronautics and Space Administration (NASA) under Grants Cooperative Agreement Notice (CAN) NNS06AA22G and Research Opportunities in Space and Earth Sciences (ROSES) NNA07CN14A. The authors also gratefully acknowledge the various sponsors and colleagues who provided support over the past years in the research, development, and refinement of both classification algorithms leading to this particular study. Paul Tag (NRL retired), for his original guidance in the development of the IP algorithm, and Andy Heidinger and Mike Pavolonis (NOAA/NESDIS ASPB), for their assistance with the EP algorithm, are specifically acknowledged here. We extend a special acknowledgment and thanks to our coauthor Dr. Robert Wade, who passed

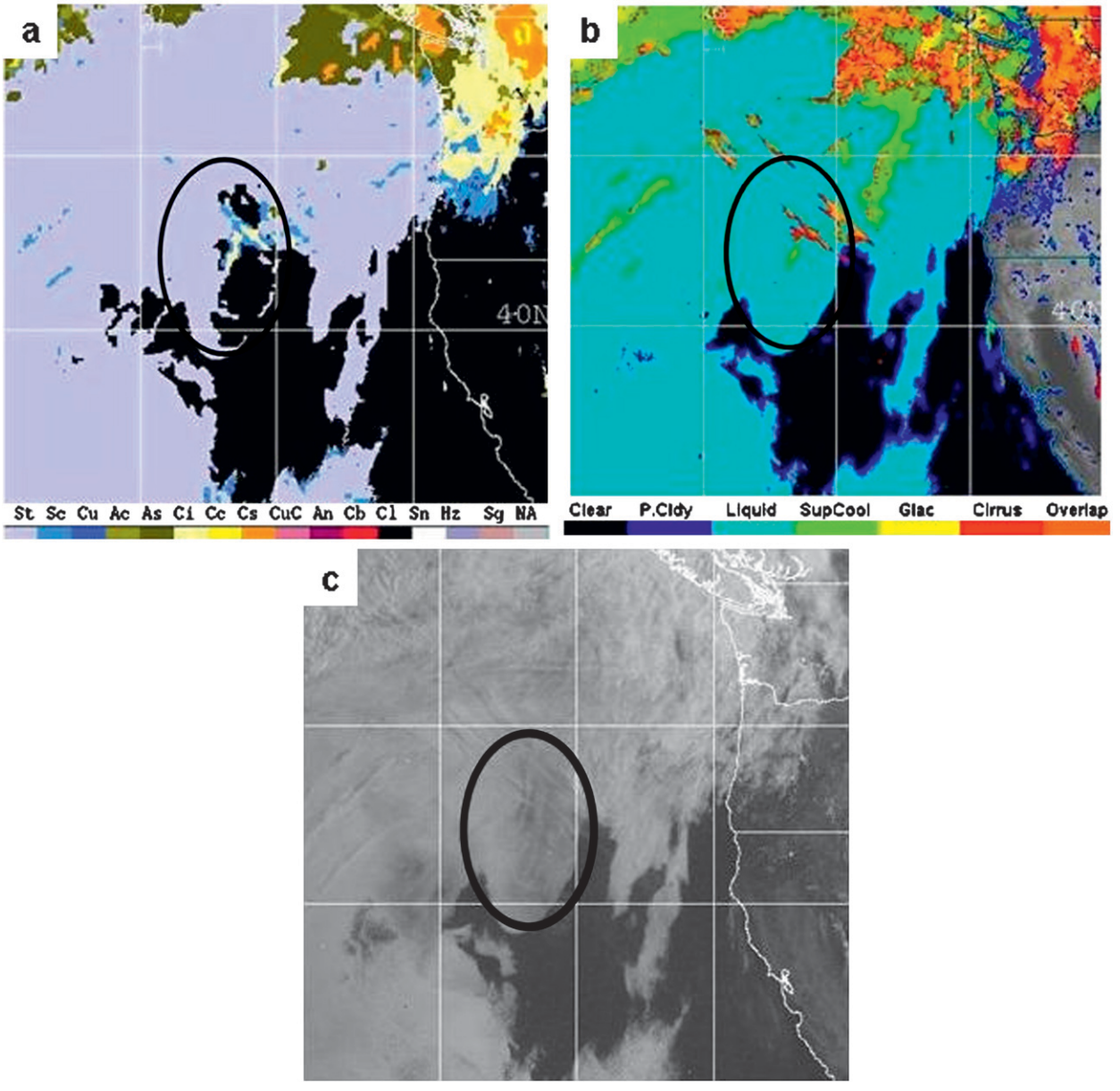

FIG. 8. Example case (1600 UTC 6 May 2007) of (a) IP classification of Clr, (b) EP classification of liquid clouds for the same pixels, and the (c) associated *GOES-11* visible image.

away prior to the completion of this manuscript. GOES data were acquired through a processing procedure at Code 7541 of the Naval Research Laboratory.

REFERENCES

Ackerman, S. A., R. E. Holz, R. Frey, E. W. Eloranta, B. C. Maddux, and M. McGill, 2008: Cloud detection with MODIS. Part II: Validation. *J. Atmos. Oceanic Technol.,* **25,** 1073–1086.

Baldwin, M. E., J. S. Kain, and S. Lakshmivarhan, 2005: Development of an automated classification procedure for rainfall systems. *Mon. Wea. Rev.,* **133,** 844–862.

Bankert, R. L., and D. W. Aha, 1996: Improvement to a neural network cloud classifier. *J. Appl. Meteor.,* **35,** 2036–2039.

——, and R. H. Wade, 2007: Optimization of an instance-based GOES cloud classification algorithm. *J. Appl. Meteor. Climatol.,* **46,** 36–49.

Baum, B. A., and Q. Trepte, 1999: A grouped threshold approach for scene identification in AVHRR imagery. *J. Atmos. Oceanic Technol.,* **16,** 793–800.

——, V. Tovinkere, J. Titlow, and R. M. Welch, 1997: Automated cloud classification of global AVHRR data using a fuzzy logic approach. *J. Appl. Meteor.,* **36,** 1519–1540.

Donovan, M. F., E. R. Williams, C. Kessinger, G. Blackburn, P. H. Herzegh, R. L. Bankert, S. Miller, and F. R. Mosher,

2008: The identification and verification of hazardous convective cells over oceans using visible and infrared satellite observations. *J. Appl. Meteor. Climatol.,* **47,** 164–184.

Dybbroe, A., K.-G. Karlsson, and A. Thoss, 2005: NWCSAF AVHRR cloud detection and analysis using dynamic thresholds and radiative transfer modeling. Part I: Algorithm description. *J. Appl. Meteor.,* **44,** 39–54.

Fouilloux, A., and J. Iaquinta, 1998: Assessment of clouds characteristics from satellite observations by means of self-organized neural networks. *Remote Sens. Environ.,* **66,** 101–109.

Heidinger, A. K., cited 2004: CLAVR-x cloud mask algorithm theoretical basis document (ATBD). [Available online at http://cimss.ssec.wisc.edu/clavr/clavrx_docs.html.]

——, and M. J. Pavolonis, 2005: Global daytime distribution of overlapping cirrus cloud from NOAA's Advanced Very High Resolution Radiometer. *J. Climate,* **18,** 4772–4784.

Hutchison, K. D., J. K. Roskovensky, J. M. Jackson, A. K. Heidinger, T. J. Kopp, M. J. Pavolonis, and R. Frey, 2005: Automated cloud detection and classification of data collected by the Visible Infrared Imager Radiometer Suite (VIIRS). *Int. J. Remote Sens.,* **26,** 4681–4706.

Kessinger, C., and Coauthors, 2009: The oceanic convection diagnosis and nowcasting system. Preprints, *16th Conf. on Satellite Meteorology and Oceanography,* Phoenix, AZ, Amer. Meteor. Soc., J8.3. [Available online at http://ams.confex.com/ams/pdfpapers/150291.pdf.]

Li, Z., J. Li, W. P. Menzel, T. J. Schmit, and S. A. Ackerman, 2007: Comparison between current and future environmental satellite imagers on cloud classification using MODIS. *Remote Sens. Environ.,* **108,** 311–326.

Mazzoni, D., M. J. Garay, R. Davies, and D. Nelson, 2007: An operational MISR pixel classifier using support vector machines. *Remote Sens. Environ.,* **107,** 149–158.

Mitrescu, C., S. Miller, and R. Wade, 2006: Cloud optical and microphysical properties derived from satellite data. Preprints, *14th Conf. on Satellite Meteorology and Oceanography,* Atlanta, GA, Amer. Meteor. Soc., P1.7. [Available online at http://ams.confex.com/ams/pdfpapers/100515.pdf.]

Mosher, F., 2002: Detection of deep convection around the globe. Preprints, *10th Conf. on Aviation, Range, and Aerospace Meteorology,* Portland, OR, Amer. Meteor. Soc., 289–292.

Parikh, J. A., J. S. DaPonte, J. N. Vitale, and G. Tselioudis, 1997: Comparison of genetic algorithm systems with neural network and statistical techniques for analysis of cloud structures in midlatitude storm systems. *Pattern Recognit. Lett.,* **18,** 1347–1351.

Pavolonis, M. J., and A. K. Heidinger, 2004: Daytime cloud overlap detection from AVHRR and VIIRS. *J. Appl. Meteor.,* **43,** 762–778.

——, ——, and T. Uttal, 2005: Daytime global cloud typing from AVHRR and VIIRS: Algorithm description, validation, and comparisons. *J. Appl. Meteor.,* **44,** 804–826.

Schmetz, J., S. A. Tjemkes, M. Gube, and L. van de Berg, 1997: Monitoring deep convection and convective overshooting with Meteosat. *Adv. Space Res.,* **19,** 433–441.

Seemann, S. W., J. Li, W. P. Menzel, and L. E. Gumley, 2003: Operational retrieval of atmospheric temperature, moisture, and ozone from MODIS infrared radiances. *J. Appl. Meteor.,* **42,** 1072–1091.

Tag, P. M., R. L. Bankert, and L. R. Brody, 2000: An AVHRR multiple cloud-type classification package. *J. Appl. Meteor.,* **39,** 125–134.

Wang, Z., and K. Sassen, 2001: Cloud type and macrophysical property retrieval using multiple remote sensors. *J. Appl. Meteor.,* **40,** 1665–1682.